

Provided for non-commercial research and education use.
Not for reproduction, distribution or commercial use.



This article appeared in a journal published by Elsevier. The attached copy is furnished to the author for internal non-commercial research and education use, including for instruction at the authors institution and sharing with colleagues.

Other uses, including reproduction and distribution, or selling or licensing copies, or posting to personal, institutional or third party websites are prohibited.

In most cases authors are permitted to post their version of the article (e.g. in Word or Tex form) to their personal website or institutional repository. Authors requiring further information regarding Elsevier's archiving and manuscript policies are encouraged to visit:

<http://www.elsevier.com/copyright>



Contents lists available at ScienceDirect

International Journal of Fatigue

journal homepage: www.elsevier.com/locate/ijfatigue

Practical fatigue analysis of hydraulic cylinders – Part II, damage mechanics approach

Tomasz Bednarek *, Włodzimierz Sosnowski

Institute of Fundamental Technological Research, Polish Academy of Sciences, ul. Pawińskiego 5b, 02-106 Warsaw, Poland

Kazimierz Wielki University, Institute of Environmental Mechanics and Applied Computer Science, ul. Chodkiewicza 30, 85-064 Bydgoszcz, Poland

ARTICLE INFO

Article history:

Received 11 September 2009

Received in revised form 6 January 2010

Accepted 24 February 2010

Available online 6 March 2010

Keywords:

Damage mechanics

Metal fatigue

Hydraulic cylinder

ABSTRACT

The paper is continuation and extension of the previous article (Marczewska et al., 2006) [1] published in Journal of Fatigue in 2006. Our previous model of analysis (Marczewska et al., 2006) [1] was based on classical S–N curves and equivalent amplitude stress concept. Now more physically justified damage mechanics approach to fatigue analysis is applied. The analysis used in both our papers is based on particular application of the constitutive model described in Oller et al. [2]. Hydraulic cylinders investigated under E.C. project “PROHIP” are analyzed. Modeling of fatigue crack propagation is performed. The new elements, in comparison with previous paper (Marczewska et al., 2006) [1] are: application of the thermodynamic basics of damage mechanics approach to fatigue analysis with taking into account plastic deformations, introduction of damage evolution surface in fatigue analysis, modification of analytical form of S–N curve proposed in Oller et al. [2] and fatigue crack propagation modeling using damage mechanics approach. As it was mentioned in Marczewska et al. [1] the “marriage” of stress analysis and fatigue data is still one of deficiencies in the current European Norm EN 13445, chapter 18: detailed assessment of fatigue life [3]. Our paper is an attempt to further reduce this deficiency.

© 2010 Elsevier Ltd. All rights reserved.

1. Introduction

From the engineering point of view forecasting of fatigue live of supporting structures or machine elements and other structural components require to find areas, where stresses in the structure are relatively high and the fatigue failure may occur. Usually this situation occur at notches, where the geometrical discontinuities lead to stress concentrations. In these weak points of the structure a detailed stress and strain analysis must be performed. As it is written at the end of European Norm EN 13445 rules description (point 18I, detailed assessment of fatigue life) [3] the ‘marriage’ of stress analysis from finite element analysis and fatigue data is still one of the deficiencies in the current EN 13445.

In 2005 Oller et al. [2] developed a constitutive material model with fatigue expansion based on work of Chaboche [4] and later [5,6]. They proposed a analytical form of S–N curves and reduction of material strength function. In this paper several new elements are introduced:

- application of thermodynamic basics of damage mechanics approach in fatigue analysis, taking into account plastic deformations,

- introduction of damage evolution surface in fatigue analysis,
- extension of damage mechanics approach in order to perform fatigue analysis of structures under random loading,
- modification of analytical form of S–N curve proposed in [2] and
- analysis of fatigue crack propagation in hydraulic cylinder using damage mechanics approach.

2. Application of thermodynamical basics of damage nature to fatigue analysis

The inelastic theories of damage and plasticity allow to solve mechanical problems with material behavior beyond the elastic range. Such kind of solutions neglect the cyclic load effects however. If we want to take such cyclic loads into account, the thermodynamic phenomena which occur in inelastic material with fatigue damage parameter should be taken into consideration.

Generally, damage parameter d is a fourth order tensor [7,8]. If we assume fully isotropic material behavior, then the damage tensor d is reduced to a scalar value d . In spite of the simplification of the nature of fatigue fracture, which is an anisotropic phenomenon, many authors apply isotropic damage parameter, for example [9,10].

The elastic part of the free energy, considering infinite small deformations and constant temperature, is equal [11]

$$\Psi^e(\epsilon_{ij}^e, d) = \frac{1}{2\rho} \left[\epsilon_{ij}^e C_{ijkl}^d(d) \epsilon_{kl}^e \right], \quad (1)$$

* Corresponding author. Address: Institute of Fundamental Technological Research, Polish Academy of Sciences, ul. Pawińskiego 5b, 02-106 Warsaw, Poland.

E-mail address: bednarek@ippt.gov.pl (T. Bednarek).

where ρ is the material density, ε_{ij}^e is elastic part of strain and C_{ijkl}^d is the fourth order constitutive tensor which takes into account the evolution of the internal parameter d [10,12]. The constitutive tensor of damaged material C_{ijkl}^d can be taken from empirical dependence [13]

$$C_{ijkl}^d = (D - d)C_{ijkl}^0 \quad (2)$$

C_{ijkl}^0 is the constitutive pure material fourth order tensor, D is the critical damage value and d describes the level of degradation of the pure material. If $d = 0$ the material is not damaged, and when $d = D$ material strength corresponds to collapse. Usually parameter D is taken as 1, in spite of fact that collapse of element may occur with much smaller value of parameter D [14]. In this paper it is assumed that $D = 1$.

After substitution of Eq. (2) into Eq. (1) we obtain the formula for elastic part of the free Helmholtz energy with internal damage parameter

$$\Psi^e = (1 - d)\Psi^{e0} = \frac{1 - d}{2\rho} \left[\varepsilon_{ij}^e C_{ijkl}^0 \varepsilon_{kl}^e \right] \quad (3)$$

where Ψ^{e0} is the elastic part of free energy without damage.

The Clausius-Duhem inequality in energetic form can be formulated as follows:

$$\Gamma = m(-\dot{\Psi} - \eta\dot{\theta}) + \sigma_{ij}\dot{\varepsilon}_{ij} - \frac{1}{\theta}q_i\nabla\theta \geq 0 \quad (4)$$

where [15,9]

$$\sigma_{ij} = \rho \frac{\partial \Psi^e}{\partial \varepsilon_{ij}^e} \quad \text{and} \quad \eta = -\frac{\partial \Psi}{\partial \theta} \quad (5)$$

η is the entropy, θ is the temperature and q_i is the vector of heat flux.

The stress value in the damaged element can be calculated by a substitution of derivatives of Ψ^e (Eq. (3)) into Eq. (4)

$$\sigma_{ij} = \rho \frac{\partial \Psi^e}{\partial \varepsilon_{ij}^e} = (1 - d)C_{ijkl}^0 (\varepsilon_{kl} - \varepsilon_{kl}^p), \quad \varepsilon_{ij} = \varepsilon_{ij}^e + \varepsilon_{ij}^p \quad (6)$$

or

$$\sigma_{ij} = (1 - d)\sigma_{ij}^0 \quad (7)$$

where σ_{ij}^0 is the stress in an undamaged element.

The second thermodynamical law indicates, that inequality (4) must be satisfied. Truesdell [11] made an assumption, that inequality (4) must be satisfied separately for mechanical and thermal parts. The mechanical part of inequality (4), which describes the mechanical energy dissipation corresponds to Planck inequality [11]

$$\Gamma_m = \sigma_{ij}\dot{\varepsilon}_{ij}^p - \rho \frac{\partial \Psi^p}{\partial \alpha} \dot{\alpha} - \rho \frac{\partial \Psi^p}{\partial d} \dot{d} \geq 0 \quad (8)$$

The process of fatigue damage evolution must satisfy conditions in Eq. (8). In the fatigue analysis of structures two kinds of energy dissipation have to be taken into account: plastic dissipation and dissipation which corresponds with fatigue degradation of material. The Planck inequality (8) is next used in Eqs. (21) and (22) in order to make damage parameter irreversible.

3. Plastic function and evolution of damage in fatigue analysis

Elastic limit is described by the yield criterion

$$F(\sigma_{ij}, \alpha) = f(\sigma_{ij}) - K(\sigma_{ij}, \alpha) \leq 0, \quad (9)$$

where $K(\sigma_{ij}, \alpha)$ is yield limit.

The scalar function $G(\sigma)$ is the plastic potential for $\dot{\varepsilon}^p$. The flow law is [15,16]

$$\dot{\varepsilon}_{ij}^p = \lambda \frac{\partial G}{\partial \sigma_{ij}}, \quad \text{where} \quad \lambda > 0, \quad (10)$$

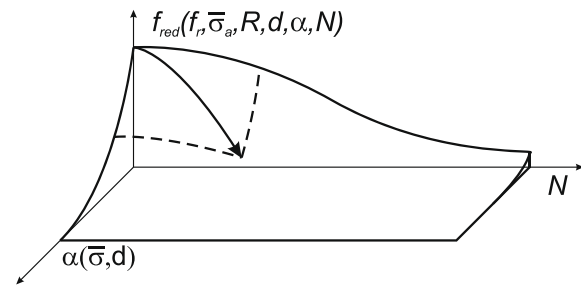


Fig. 1. Yield – damage evolution surface [2].

λ is the scalar function. If we assume, that plastic potential G is identified with the flow function f , Eq. (10) will represent the associated flow law and

$$\dot{\varepsilon}_{ij}^p = \lambda \frac{\partial f}{\partial \sigma_{ij}}, \quad \text{where} \quad \lambda > 0 \quad (11)$$

In an analogy to the associated flow law, a material fatigue strength limit can be build [2].

$$F^D(\sigma_{ij}, d, \alpha, R) = \bar{\sigma}(\sigma_{ij}, d, \alpha) - f_r(R) \cdot f_{red}(N, \bar{\sigma}_a, R, d) \leq 0, \quad (12)$$

where $\bar{\sigma}$ is the equivalent stress (i.e. Huber–von Mises stress) in the damaged element, f_r is the fatigue endurance limit and f_{red} is the reduction of material strength function. Reduction of the material strength function f_{red} depends on the stress history (number of cycles loading–unloading), amplitude of equivalent stress $\bar{\sigma}_a$ and the stress ratio R . Similarly like in the case of theory of plasticity, an evolution of damage parameter is given by equations [9,10,2]

$$\dot{d} = \mu \frac{\partial F^D}{\partial \sigma}, \quad \dot{d} \geq 0 \quad (13)$$

where μ has similar properties to λ .

The mechanical and damage processes described above allow to define a fatigue limit surface. The fatigue limit surface, presented in Fig. 1, depends on the plastic effects of deformation. The process of degradation of material strength is limited by the fatigue limit surface and it allows to simulate propagation of fatigue damage during the load history.

4. Reduction of material strength function by brittle parameter

In 2005 Oller proposed an analytical form of fatigue S–N curve [2]. Such form of S–N surface allows to use Goodman theory of mean stress influence on fatigue [17]. Authors propose a modified analytical form of fatigue S–N function as follows [1]:

$$S_N(R, N) = S_{th}(R) + [S_u - S_{th}(R)] \times 10^{[-\alpha_t(R) \cdot \log(N)^\beta]} \quad (14)$$

where

$$\left. \begin{aligned} S_{th}(R) &= S_e + (S_u - S_e) \cdot (0.5 + 0.5R)^\gamma \\ \alpha_t(R) &= \alpha + (0.5 + 0.5R) \cdot \delta \end{aligned} \right\} \quad \text{for} \quad |R| \leq 1$$

$$\left. \begin{aligned} S_{th}(R) &= S_e + (S_u - S_e) \cdot (0.5 + \frac{1}{2R})^\gamma \\ \alpha_t(R) &= \alpha + (0.5 + \frac{1}{2R}) \cdot \delta \end{aligned} \right\} \quad \text{for} \quad |R| > 1 \quad (15)$$

S_u is the material tensile strength, $\alpha, \beta, \gamma, \delta$ are the material parameters, S_{th} is the fatigue threshold function depending on the endurance fatigue stress S_e and the stress ratio R .

A modification of the S–N function formulas developed by Oller [2] is done in order to get a full agreement of the presented method with the classical S–N curves. The introduced correction also takes into account an influence of mean stress value σ_{mean} and the stress

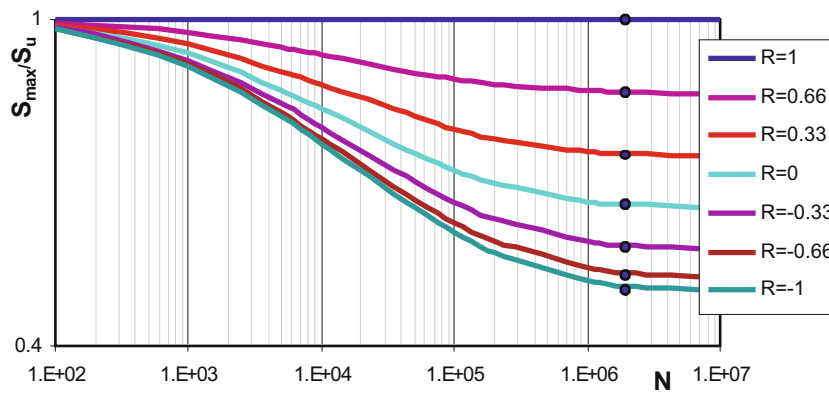


Fig. 2. The proposed S–N curves for different R values.

ratio R on fatigue life of the structure and agrees with Goodman's concept [1].

In Fig. 2 the proposed S–N functions are presented. The influence of the stress ratio R is shown. The bold points indicate fatigue threshold values calculated by Goodman's concept. After transformation of Eq. (14) and substitution of the stress from FEM analysis $\bar{\sigma} \equiv S(N, R)$, we obtain the fatigue life of the structure. Fatigue life is expressed as a number of cycles to failure N_{cyc} . Transformation of formula (14) gives

$$N_{cyc}(R, \bar{\sigma}) = 10 \left[\left(\frac{\log \left(\frac{S_u - S_{th}(R)}{\bar{\sigma} - S_{th}(R)} \right)}{a_t(R)} \right)^\beta \right] \quad (16)$$

The S–N curve determined by Eqs. (14) and (16) allows to determine fatigue life of the structure where the load is characterized by constant amplitude and constant stress ratio. It is observed that during fatigue crack propagation consecutive material points are damaged (separated) along a crack. In order to describe evolution of fatigue crack authors introduce a modification of a material strength reduction function, originally presented by Luccioni and Oller [9,2].

We propose introduction of a material brittle parameter m which controls the evolution of fatigue crack.

$$f_{red}(\bar{\sigma}, R, N) = 10^{\frac{\log \left(\frac{\bar{\sigma}}{S_u} \right)}{\log(N_{cyc})^{\beta m}} \log(N)^{\beta m}} \quad (17)$$

In Fig. 3 reduction of material strength function for different parameters m is presented.

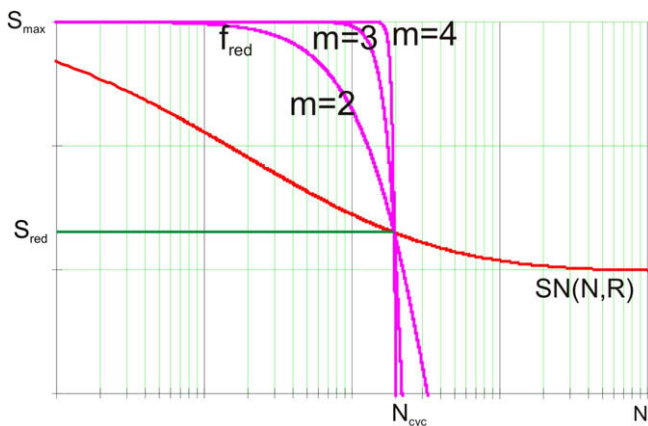


Fig. 3. Proposed strength reduction function for different m values.

The strength reduction function is identified with damage of material point $f_{red}(\bar{\sigma}, R, N) \equiv 1 - d$, in that case Eqs. (2) and (6) can be rewritten as

$$\begin{aligned} C_{ijkl}^d &= f_{red}(\bar{\sigma}, R, N) C_{ijkl}^0 \\ \sigma_{ij} &= f_{red}(\bar{\sigma}, R, N) \sigma_{ij}^0 \end{aligned} \quad (18)$$

Furthermore

$$S_{ud} = f_{red}(\bar{\sigma}, R, N) S_u \quad (19)$$

where S_{ud} is the damaged material strength.

When load history (or response of structure) is not regular, stress amplitude, mean stress and stress ratio are not constant. In such a complex situation simplified damage mechanics concept presented above can not be applied. It is necessary to obtain fatigue crack increment per cycle. After differentiation of Eq. (17) with respect to N we obtain

$$\frac{\partial f_{red}(S_{red}, R, N)}{\partial N} = f_{red}(S_{red}, R, N) \frac{\beta^m \cdot \log \left(\frac{S_{red}}{S_u} \right) \cdot \log(N)^{\beta m - 1}}{N \cdot \log(N_{cyc})^{\beta m}} \quad (20)$$

Eq. (20) is used in fatigue analysis when applied load or response of the structure are not regular (for instance inelasticity, dynamics, random load). It is necessary to build fatigue analysis iterative loop in which fatigue damage contribution from single load–unload cycle (or group of cycles) can be added. Eq. (21) allows to perform fatigue analysis of structures with irregular response.

$$f_{red}^{(t+1)}(S_{red}, R, N) = f_{red}^{(t)}(S_{red}, R, N) + N_{blk} \frac{\partial f_{red}(S_{red}, R, N)}{\partial N} \quad (21)$$

where N_{blk} is number of cycles i cycle block and upper index (t) means iteration number. It is interesting that second term on the right hand side of Eq. (21) takes negative values

$$\frac{\partial f_{red}(\bar{\sigma}, R, N)}{\partial N} \leq 0 \quad (22)$$

which satisfies Clausius-Duhem inequality (8).

5. Numerical example – a fatigue numerical analysis of hydraulic cylinder oil port zone versus experiment

Fatigue damage of the hydraulic cylinder, shown in Figs. 4 and 5, was investigated experimentally in [18,19]. The same cylinder was chosen for our research in order to illustrate fatigue numerical analysis based on damage mechanics concept. Fatigue experiments of the hydraulic cylinder were performed within the European project PROHIPP coordinated by Pedro Roquet SA [19,18].

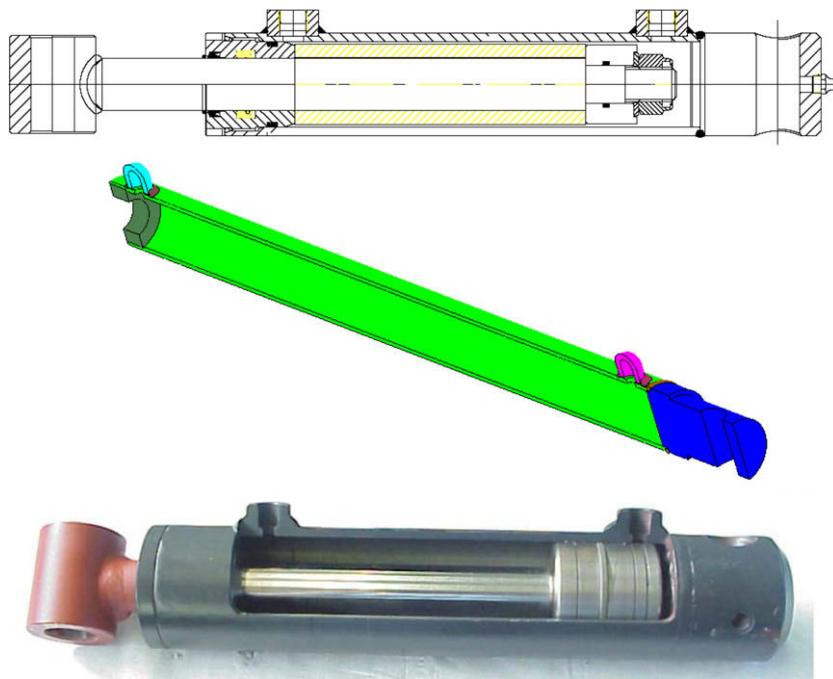


Fig. 4. Technical sketch, model and section of the hydraulic cylinder [19].



Fig. 5. Pictures of the tested hydraulic cylinders [18].

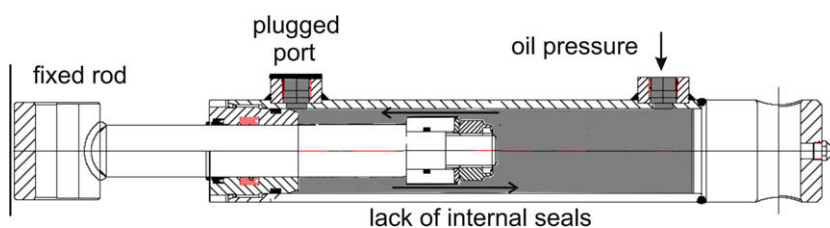


Fig. 6. The schematic sketch of the hydraulic cylinder test stand.

The numerical analysis is divided into two parts. First the fatigue resistance of the cylinder was calculated and compared with experiment. The second part corresponds to simulation and visualization of fatigue crack propagation. These results were compared with experiment as well.

5.1. Calculation of fatigue resistance of the hydraulic cylinder using FEM and equivalent amplitude stress concept

The cylinder, shown in Fig. 4, has two oil ports and was made from St52 steel. The material parameters are as follows: density $\rho = 7800 \text{ kg/m}^3$, Young modulus $E = 210 \text{ GPa}$, Poisson coefficient $\nu = 0.3$, yield stress $S_y = 350 \text{ MPa}$ and ultimate stress $S_u = 600 \text{ MPa}$.

The welds and the virgin material of the hydraulic cylinder are the same.

The fatigue tests were performed under test load. The test load does not correspond to real loads of the working hydraulic cylinders and was adopted by Pedro Roquet SA [19,18] in order to perform fast, cheap and reliable fatigue experiments of the hydraulic cylinders.

The cylinder was attached to the stand by belts. The piston of hydraulic cylinder was fixed. The internal seals are removed. So the free flow of the fluid between both sides of the piston is allowed. One of the oil ports was plugged and to the other oil under pressure was supplied. The schematic sketch of the test stand is presented in Fig. 6.

The oil pressure inside cylinder oscillated between 0 bar and 306 bar with accuracy ± 2 bar ($0\text{--}30.6$ MPa, ± 0.2 MPa). The oscilloscope chart of the oil pressure is presented in Fig. 7. In numerical analysis the maximum test value of oil pressure was assumed as 30.8 MPa and stress ratio $R = 0$.

The following material fatigue parameters were assumed: fatigue endurance limit $S_e = 200$ MPa, S–N curve coefficients (see Eqs. (14) and (15) and Fig. 9) $\alpha = 0.00085$, $\beta = 3.5$, $\gamma = 3.0$, $\delta = -0.0004$ and the exponent $m = 2$.

During the analysis 10 critical zones, presented in Fig. 8, were identified. Zones number 1 and 2 correspond to the weld between cylinder tube and the end cap, zones number 3–6 correspond to oil port (near end cap) and zones number 7–10 correspond to rod oil port. The stress analysis of the cylinder was performed by finite element method program FEAP by Taylor [20]. The reduced von Mises

stress values in critical zones are as follows: zone 1 – 387.2 MPa, zone 2 – 321.2 MPa, zone 3 – 357.0 MPa, zone 4 – 208.5 MPa, zone 5 – 248.3 MPa, zone 6 – 345.5 MPa, zone 7 – 366.9 MPa, zone 8 – 243.5 MPa, zone 9 – 221.4 MPa and zone 10 – 372.3 MPa.

The fatigue resistance of the hydraulic cylinder was established as a number of load–unload cycles to failure. The number of cycles to failure was calculated using formula (16). The graphical interpretation of the fatigue resistance calculation for each critical zone is presented in Fig. 9.

The deformation and stress fields of the hydraulic cylinder are shown in Fig. 10.

The results of the stress and fatigue resistances, presented in Table 1, were divided into three sections: end cap weld, oil port I (near end cap) and oil port II (port rod). The division of results corresponds to the experimental data. We have only information

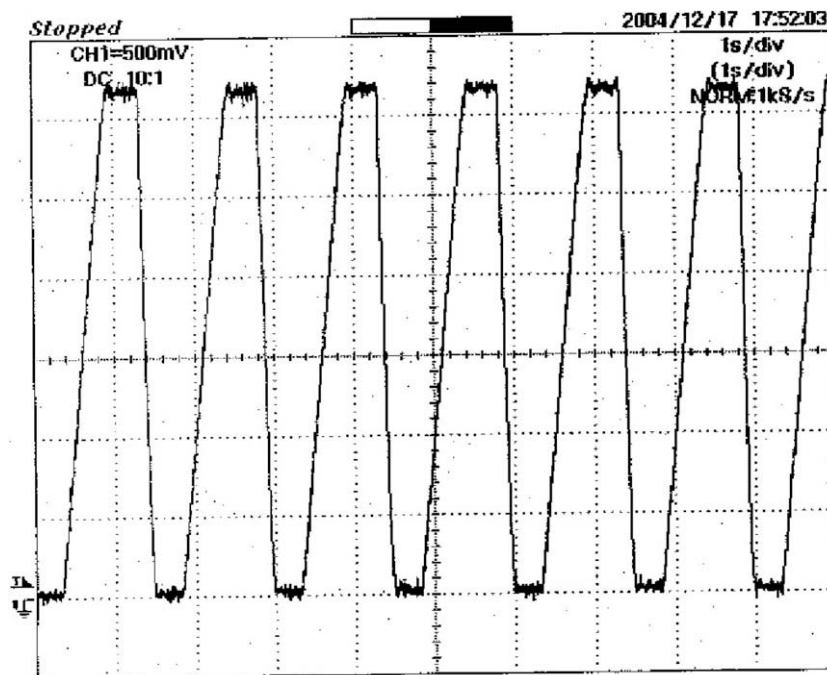


Fig. 7. The oscilloscope chart of the oil pressure inside the hydraulic cylinder [18].

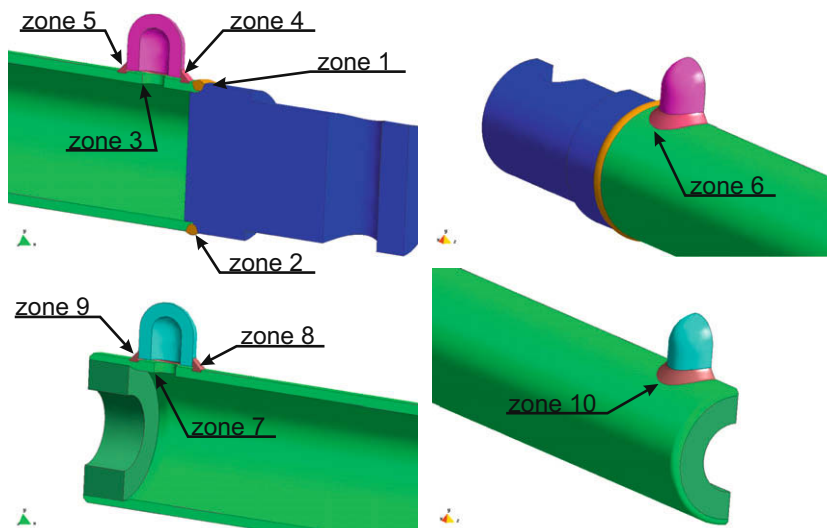


Fig. 8. Critical zones of the hydraulic cylinder.

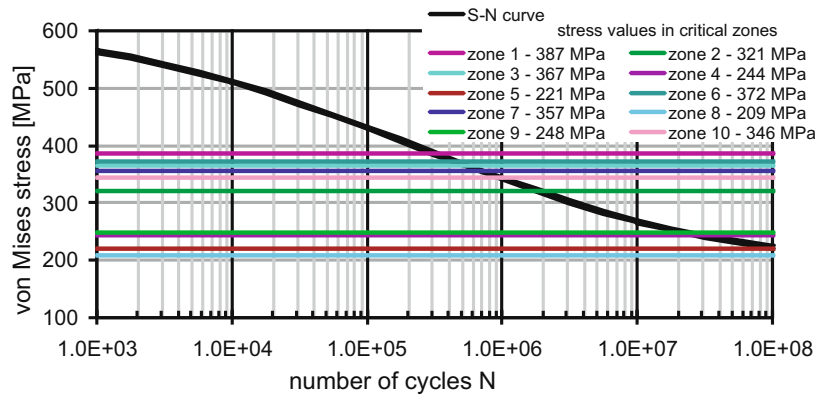


Fig. 9. The S–N curve with stress values in critical zones.

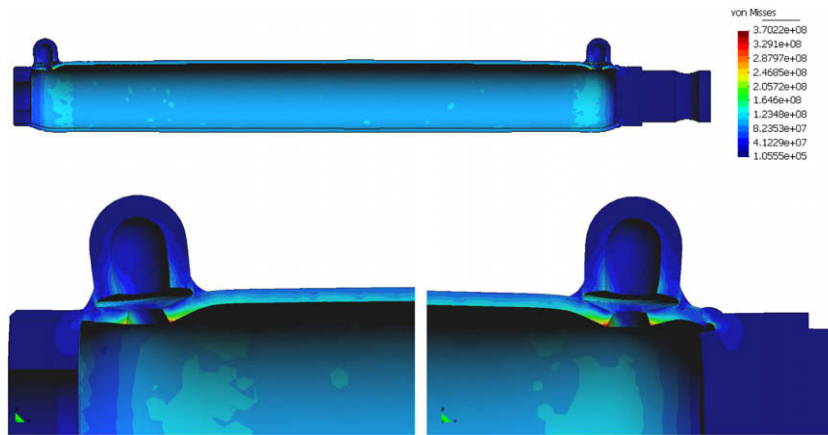


Fig. 10. The reduced von Mises stress field on deformed hydraulic cylinder. Deformation scale coefficient 500.

where the leakage occur. In other words in experimental test we do not know which critical zone is the weakest, we know only where the leakage occur. Numerical calculations allows to find very accurately point of maximum stress value.

The conclusion of the fatigue experiments of hydraulic cylinder is that the weakest elements of the cylinder are end cap weld and the oil port I (near end cap). The numerical calculations confirm this fact. The weakest zone is the zone number 1 (end cap weld) with fatigue resistance 309719 cycles and corresponds to experimental values of 350395–384000 cycles. In case of oil port near end cap the weakest fatigue resistance zones are zone 3 and zone 6. The fatigue resistances are 520395 and 452944 cycles respec-

Table 1
Comparison of calculated and real fatigue resistance of the hydraulic cylinder.

Critical zone	Stress value (MPa)	Fatigue resistance, calculation (number of cycles)	Fatigue resistance, experiment [18] (number of cycles)
Weld between cylinder tube and end cap	1	387.2	384000
	2	321.2	352249 350395
Oil port I	3	366.9	436887
	4	243.5	>5000000 598798
	5	221.4	>5000000 347427
	6	372.3	452944 358947
Oil port II	7	357.0	672740 675891
	8	208.5	>5000000 581900
	9	248.3	>5000000 740698
	10	345.5	911011 763187

tively and correspond to experimental values of fatigue live from 358947 to 598794 cycles.

The number of experimental tests is not sufficient to obtain reliable values of fatigue life of the cylinder. The differences between experimental and estimated by numerical calculations fatigue resistances are relatively small.

5.2. Analysis of fatigue crack growth using damage mechanics approach

The fatigue analysis of hydraulic cylinder using damage mechanics was made. This method allows to indicate zones where fatigue cracks were initiated. Additionally damage mechanics approach allows to observe the direction and velocity of fatigue crack growth.

The fatigue crack growth investigation is limited to the area of the oil port near end cap. Numerical example of fatigue analysis using damage mechanics approach illustrate the process of fatigue crack propagation. Cylinders tested within project PROHIPP were cut and the fatigue cracks were measured and analyzed. Additionally fatigue cracks which do not cause leakage were also analyzed (see Fig. 14).

The field of reduced von Mises stress in the oil port area (zones 3–5) is presented in Fig. 11.

Consecutive phases of fatigue crack propagation in oil port area are presented in Fig. 12 (zones 3–5) and in Fig. 13 (zone 6). It can be observed that the fatigue crack was initiated on internal side of the cylinder near hole in the cylinder tube (zone 3, Fig. 12). Next,

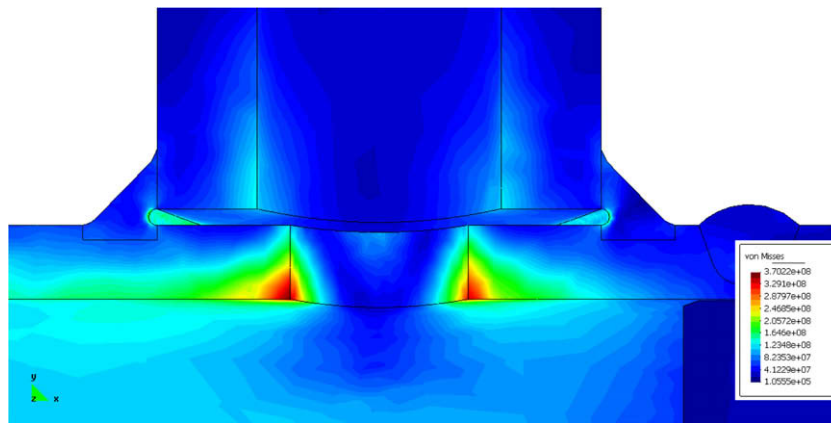


Fig. 11. Reduced von Mises stress field – oil port area.

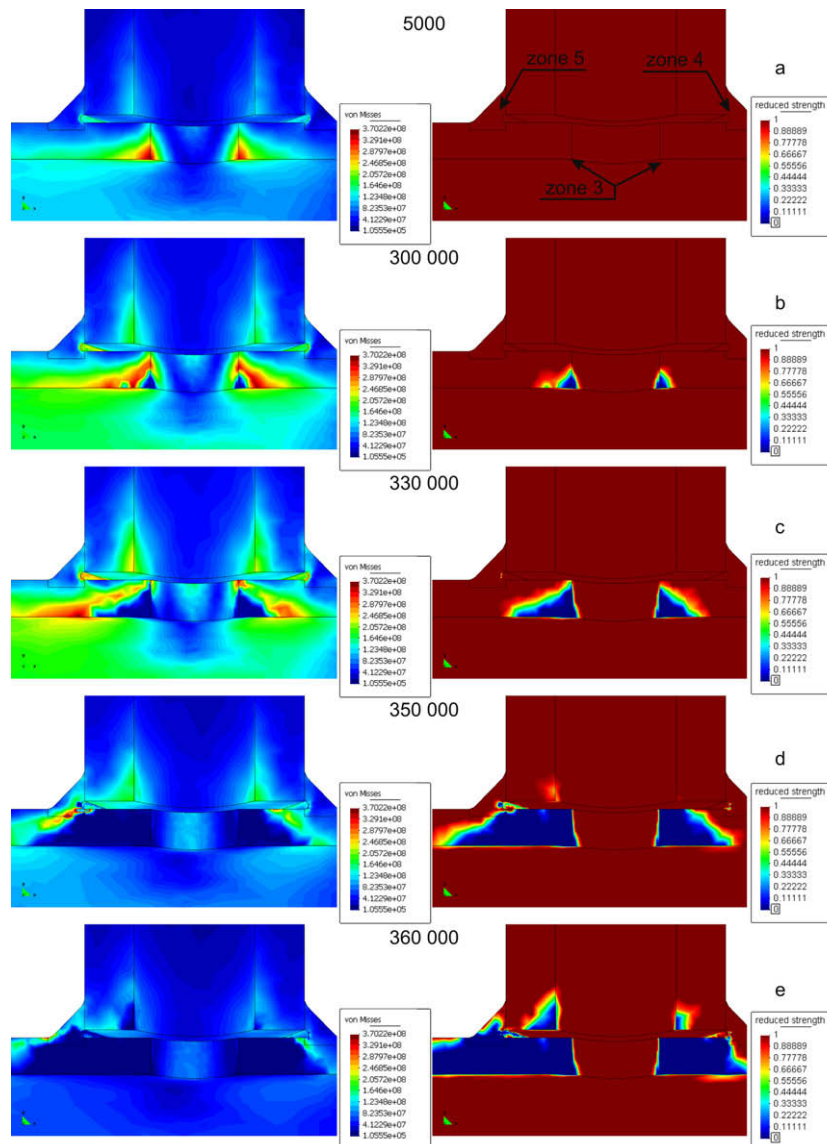


Fig. 12. The evolution of the von Mises stress field (left hand side) and the damage parameter (right hand side). Parallel to the cylinder axis plane, critical zones 3–5.

the fatigue crack propagates along cylinder axis, breaks the weld between cylinder tube and oil port (zone 5) and finally causes

the leakage in zone 5. Similar behavior of structure crack can be observed in zone 4 (Fig. 12).

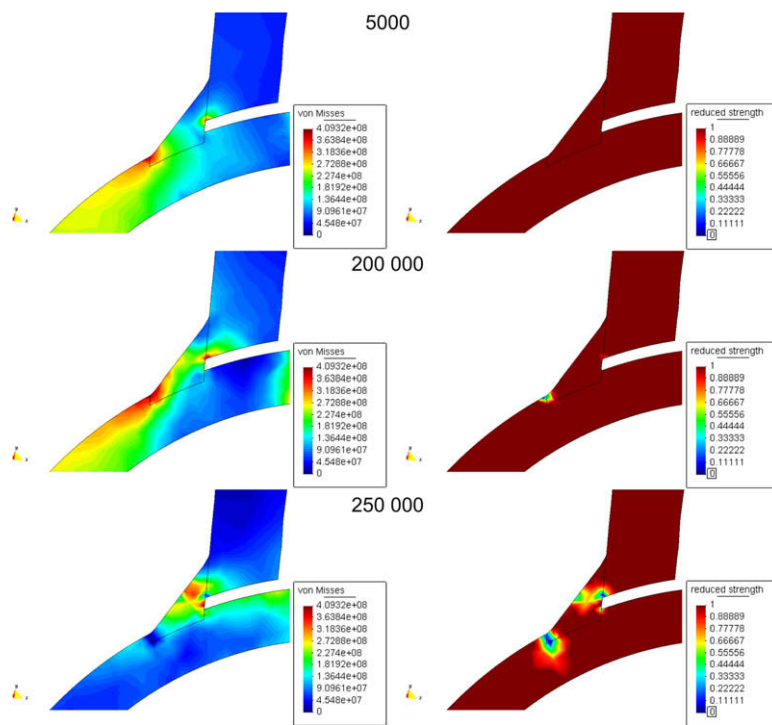


Fig. 13. The evolution of the von Mises stress field (left hand side) and the damage parameter (right hand side). Perpendicular to the cylinder axis plane, critical zone 6.

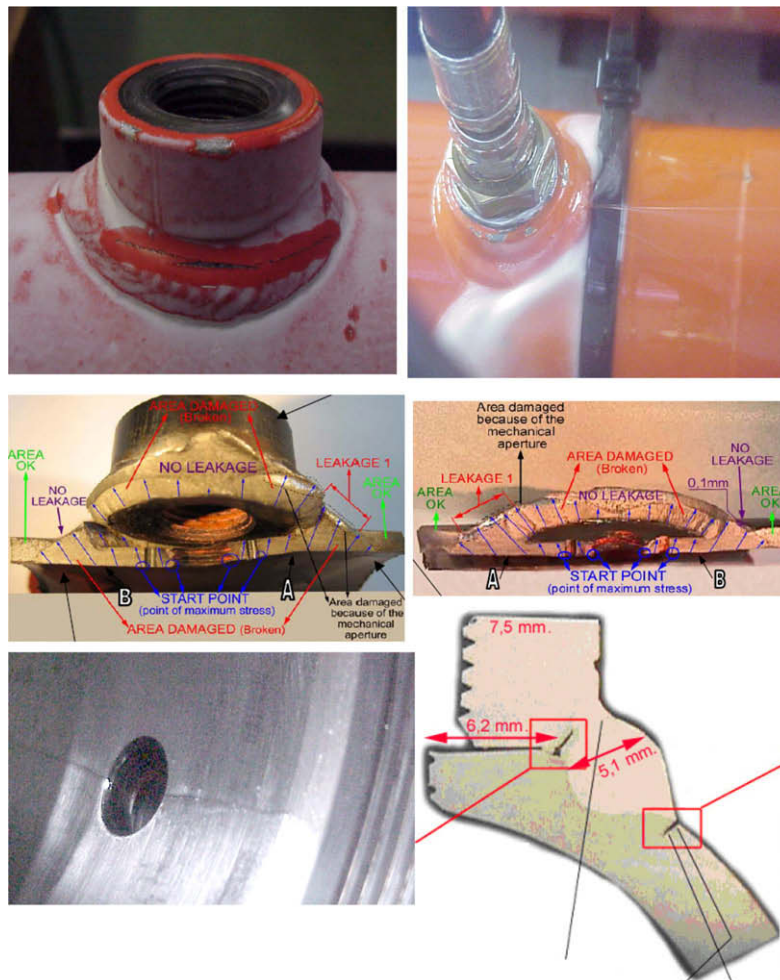


Fig. 14. Pictures of the tested cylinders and their sections [18,19].

Table 2
Table of indexes.

Report	Explanation
∇	Nabla operator
ρ	Density
E	Young modulus
ν	Poisson ratio
σ_0	Initial flow stress
p	Inner pressure
N	Number of cycles
Ψ	Free Helmholtz energy
Ψ^e	Free Helmholtz energy, elastic part
Ψ^p	Free Helmholtz energy, plastic part
ε_{ij}^e	Strain tensor, elastic part
ε_{ij}^p	Strain tensor, plastic part
C_{ijkl}^0	Constitutive tensor, pure material
C_{ijkl}^d	Constitutive tensor, damaged material
D	Critical damage value
d	Damage
θ	Temperature
\mathbf{q}_i	Vector of heat flux
η	Entropy
σ_{ij}	Stress tensor
σ_{ij}^0	Stress tensor, undamaged material
Γ	Energy dissipation
Γ_m	Energy dissipation, mechanical part
Γ_θ	Energy dissipation, thermal part
G	Plastic potential
λ, μ, f	Scalar functions
F^D	Fatigue strength limit
$\bar{\sigma}$	Equivalent stress
f_r	Fatigue endurance limit
f_{red}	Reduction of material strength function
SN	Stress of S–N function
S_{th}	Threshold stress
S_u	Ultimate stress
S_u^d	Ultimate stress of damaged material
$\alpha, \beta, \gamma, \delta$	Material parameters
R	Stress ratio
N_{cyc}	Number of cycles to failure
S_y	Yield stress
m	Material brittle measure

The character of fatigue crack growth in zone 6 (Fig. 13) is slightly different. The fatigue crack in zone 6 was initiated on the external side of the cylinder tube. The direction of the crack propagation is perpendicular to the cylinder tube wall.

Results of investigation of fatigue cracks propagation using FEM with implemented damage mechanics approach were confirmed by observations of the sections of the tested cylinders in experiment. The sections of the hydraulic cylinders tested in experiment are presented in Fig. 14.

The leakage occurs after 360 000 cycles in zone 5 (see Fig. 12e). In experiments fatigue resistance of oil port area ranges from 347 427 to 598 798 cycles.

Fatigue life of oil port area obtained by damage mechanics approach is slightly closer to experimental fatigue life than that obtained by classical S–N method (452 944 cycles). Numerical simulation of crack propagation require much more computational effort than classical fatigue or stress analysis however, because fatigue analysis using damage mechanics is an iterative process. On each step of calculation the main FEM system of equations must be solved and stress and damage fields must be calculated.

The set of indexes used in this paper is presented in Table 2.

6. Conclusions

- Damage mechanics in fatigue analysis allows to take into account interactions between elastic and plastic material

behavior. This is not possible when classical S–N method with equivalent amplitude stress concept is used.

- The damage mechanics approach in fatigue analysis allows to simulate crack initiation and propagation. Obtained results of fatigue resistance are closer to experimental values of fatigue life, than above mentioned S–N method.
- Knowledge about localization, direction and propagation speed of fatigue crack provides data for optimization of structure.
- Fatigue analysis using damage mechanics approach demands much more computational effort than classical S–N analysis. Both methods are complementary however in the sense that should give similar results. Damage mechanics approach may be used as alternative for validation of numerical studies on fatigue life of structures.

Acknowledgements

“PROHIPP” project is partially funded by the E.C. inside the sixth framework programme, priority 3 NMP FP62002-NMP-2-SME, Research area 3.4.3.1.5: support to the development of new knowledge based added value products and services in traditionally less RTD intensive industries.

We thanks the financial contribution of the E.C. and we state that the article reflects only the personal opinion of the authors.

Authors are indebted to the Roquet SA and to CIMNE for providing experimental data used in these calculations.

References

- [1] Marczevska I, Bednarek T, Marczevski A, Sosnowski W, Jakubczak H, Rojek J. Practical fatigue analysis of hydraulic cylinders and some design recommendations. *Int J Fatigue* 2006;28:1739–51.
- [2] Oller S, Salomón O, Onate E. A continuum mechanics model for mechanical fatigue analysis. *Comput Mater Sci* 2005;32(2):175–95.
- [3] European Norm EN 13445. Unifired pressure vessels [chapter 18: detailed assessment of fatigue life]. <<http://www.unm.fr/en/general/en13445/default.htm>>.
- [4] Chaboche JL. Une loi differentielle d'endommagement de fatigue avec cumulation non lineaire. *Revue Francaise de Mecanique* 1974;50–51:0.
- [5] Chaboche JL. Continuum damage mechanics: part i – general concepts. *J Appl Mech* 1988;55:59–64.
- [6] Chaboche JL. Continuum damage mechanics: part ii – damage growth, crack initiation and crack growth. *J Appl Mech* 1988;55:65–72.
- [7] Cauvin A, Testa R. Elastoplastic material with isotropic damage. *Int J Solids Struct* 1999;36:727–46.
- [8] Cauvin A, Testa R. Damage mechanics: basic variables in continuum theories. *Int J Solids Struct* 1999;36:747–61.
- [9] Luccioni B, Oller S, Danesi R. Coupled plastic-damaged model. *Comput Methods Appl Mech Eng* 1996;129:81–9.
- [10] Lemaitre J. A course on damage mechanics. Berlin: Springer-Verlag; 1992.
- [11] Truesdell C. A first course in rational continuum mechanics, vol. 1. Baltimore; 1972.
- [12] Chaboche JL. Continuum damage mechanics and its application to structural lifetime prediction. *Rech Aerosp* 1987;4:37–54.
- [13] Kachanov L. Time of the rupture process under creep conditions. *IVZ Akad Nauk SSR, Otd Tech Nauk* 1958;8:26–31.
- [14] Szala J. Hipotezy sumowania uszkodzeń zmoczeniowych. Bydgoszcz: Wydawnictwo Uczelniane ATR; 1998 [in polish].
- [15] Sosnowski W. Symulacja numeryczna, analiza wrażliwości i optymalizacja nieliniowych procesów deformacji konstrukcji (Numerical simulation, sensitivity analysis and optimization of nonlinear deformations of structures). Bydgoszcz: Wydawnictwo Akademii Bydgoskiej; 2003 [in polish].
- [16] Ostrowska-Maciejewska J. Mechanika ciał odkształcalnych (Mechanics of dermable bodies). Warszawa: PWN; 1994 [in polish].
- [17] Frost N, Marsh K, Pook L. Metal fatigue. Mineola, New York: Dover Publications, Inc.; 1999.
- [18] JimTnez G. Summary of static fatigue tests. Tech. rep., PROHIPP-01-024-001; 2005.
- [19] Carbonell M. Update of the crack analysis in fatigue tests for the cylinders. Tech. rep., PROHIPP-01-133-001; 2007.
- [20] Taylor RL. FEAP – a finite element analysis program. User manual, Department of Civil and Environmental Engineering, University of California, Berkeley; 2002.